Organic Electronics 52 (2018) 309–316

Contents lists available at ScienceDirect

Organic Electronics

journal homepage: www.elsevier.com/locate/orgel

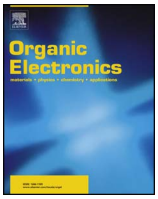

Enhanced *p-i-n* type perovskite solar cells by doping AuAg@AuAg core-shell alloy nanocrystals into PEDOT:PSS layer

Ziqi Sun[a], Yujiao Xiahou[b], Tiantian Cao[a], Kaicheng Zhang[a], Zhaowei Wang[a], Peng Huang[a], Kai Zhu[a], Ligang Yuan[a], Yi Zhou[a], Bo Song[a,**], Haibing Xia[b,***], Ning Chen[a,*]

[a] *Laboratory of Advanced Optoelectronic Materials, College of Chemistry, Chemical Engineering and Materials Science, Soochow University, Suzhou 215123, P.R. China*
[b] *State Key-Laboratory of Crystal Materials, Shandong University, Jinan 250100, P.R. China*

ARTICLE INFO

Keywords:
Perovskite solar cells
Hole transport layer
Core-shell alloy nanocrystals
AuAg@AuAg
Light-harvesting
Charge transport

ABSTRACT

Metal nanocrystals have shown great potential in the application of solar cell devices, which is ascribed to their enhancement in light-harvesting, due to the plasmonic effects. Herein, we applied AuAg@AuAg (AuAg) core-shell alloy nanocrystals (ANCs) into PEDOT:PSS layer of the *p-i-n* perovskite solar cells (pero-SCs) as dopant for the first time. The devices based on AuAg ANCs doped PEDOT:PSS reached a champion power conversion efficiency of 16.76%, showing a 28% increase compared with that of the devices based on non-doped PEDOT:PSS (13.14%). Further device characterizations, including incident photon-to-current efficiency, UV–vis absorption spectra, photoluminescence and alternating current impedance spectroscopy, suggested that the significant increase of device performance could mainly attribute to better light harvesting by the scattering effect of AuAg ANCs and better charge transport of the modified PEDOT:PSS layer. This study provides a new doping material in PEDOT:PSS to enhance the light harvesting, which leads to a significant improvement on the performance of pero-SCs.

1. Introduction

Organic-inorganic metal halide perovskite solar cells (pero-SCs) have become a research hotspot due to the advantages of high power conversion efficiency (PCE) and low fabrication cost in recent years [1–3]. Perovskite was first applied into dye-sensitized solar cells (DSSCs) as sensitizer, and the corresponding device obtained a moderate PCE of 3.8% [4]. Since then, the rapid development in this field had pushed the PCE of pero-SCs to a stunning 22.1% [5]. It is widely acknowledged that the high PCE of pero-SCs is closely related to the long exciton diffusion length and exciton lifetime [6,7], high absorption coefficient [8,9], and better carrier mobility of perovskite materials [10–12].

Many efforts, such as controllable interfacial engineering [10,13–18], perovskite film deposition [19–21] and novel device architectures [22–24], had been made to obtain higher device performance. Among them, interfacial modification had been proven to be a simple but effective approach [25]. In *p-i-n* type pero-SCs, hole transport layer (HTL) clings to the bottom electrode, and carries out the collection and transportation of charge carriers produced in the perovskite photoactive layer. So far, promising PCEs have been achieved in *p-i-n* type pero-SCs based on different HTLs, such as poly (3, 4-ethylenedioxylenethiophene):polystyrene sulfonic acid (PEDOT:PSS) [26], poly-triarylamine derivatives [27], NiO_x [28], and CuI [29].

Metal nanocrystals had been used as the dopant into HTL or photoactive layers in organic solar cells and pero-SCs and were found to be promising materials to improve the PCE of solar cells [30–45]. This PCE improvement can be ascribed to the enhanced light harvesting resulted from the localized surface plasmon resonance (LSPR) effect, which is excited on the metal surface under the light illumination. These nanocrystals served as scattering centers and sub-wavelength antennas where the absorption factor of the active medium surrounding the nanocrystals could be greatly improved by the confined electromagnetic energy based on LSPR [46]. Further studies showed that the size, shape, and composition of metal nanocrystals had a significant influence on this LSPR effect [47,48]. Initially, the nanocrystals were mainly applied to HTL of organic solar cells. For example, gold and silver dual nanocrystals have been incorporated into PEDOT:PSS layers and used as HTL in organic solar cells, leading to a 20% enhancement of PCE [47]. Recently, the nanocrystal doping strategy had also been applied into pero-

---

[*] Corresponding author.
[**] Corresponding author.
[***] Corresponding author.
E-mail addresses: songbo@suda.edu.cn (B. Song), hbxia@sdu.edu.cn (H. Xia), chenning@suda.edu.cn (N. Chen).

https://doi.org/10.1016/j.orgel.2017.11.013
Received 28 August 2017; Received in revised form 8 November 2017; Accepted 8 November 2017

SCs to improve the photovoltaic performance of the devices. Liao et al. reported about 19% improved PCE of pero-SCs by incorporating sliver nanocrystals into PEDOT:PSS layers [49]. Dai et al. systemically studied the effect of varied nanocrystals including Au, Ag, and AuAg alloy embedded into electron transport TiO_2 layer on the performance of pero-SCs, which indicated that the device performance was related to the size and synthetic method of nanocrystals and that the improvement of PCE obtained with alloy nanocrystals were better than the single nanocrystals [50].

Recently, we reported the successful synthesis of novel AuAg@AuAg (AuAg) core-shell (CS) alloyed nanocrystals (ANCs) with the beneficial properties of monodisperse, adjustable size, as well as one-step synthesis at low-temperature conditions [51]. In this work, we applied these AuAg ANCs into the PEDOT:PSS layer of *p-i-n* type pero-SCs for the first time. After the doping, device performance was improved by extending the optical pathway of incident light that increased the light absorption of perovskite layer resulted from the excellent scattering effect and better charge transport of the modified PEDOT:PSS layer. Systematic studies of device physics showed that the incorporation of AuAg ANCs led to a better light harvesting, a smoother surface morphology of the perovskite film, as well as a better charge transfer from perovskite to anode. The champion PCE of 16.76% was obtained, which was a 28% improvement compared with the control device without AuAg ANCs.

2. Experimental section

2.1. Materials

All the solvents used in the experiments were bought from Sigma Aldrich (USA). ITO glass slides with sheet resistance of ∼10 Ω/sq were bought from CSG Holding Co., Ltd. (China). The AuAg ANCs were synthesized according to the literature by a simple, Fe^{2+}-assisted, citrate co-reduction method in a one-pot reaction manner [51]. $PbCl_2$ (99.999%) and $PC_{61}BM$ were purchased from Alfa Aesar (USA) and American Dye Source, Inc. (Canada), respectively. 1, 8-diiodooctane (DIO) was acquired from TCI Development Co., Ltd. (Shanghai).

2.2. Preparation of $MAPbI_{3-x}Cl_x$ perovskite precursor

The synthesis of methylammonium iodide (MAI) was referred to a previous literature [52]. The MAI was synthesized by mixing hydroiodic acid (57 wt%, in water) (20 mL) and methylamine (33 wt%, in ethanol) (15 mL) at 0 °C for 2 h. The crude product was obtained by reduced pressure distillation, and then the product was recrystallized by dissolving in anhydrous ethanol and precipitating in anhydrous diethyl ether for 3 times, and dried at 50 °C for 24 h in vacuum drying oven. The $MAPbI_{3-x}Cl_x$ precursor (40 wt%) was prepared by mixing $PbCl_2$ and MAI in a 1:3 M ratio in anhydrous *N,N*-dimethylformamide (DMF, 99.8%) and stirred at 60 °C. After ∼30 min, 1 wt% of DIO was added to the $MAPbI_{3-x}Cl_x$ precursor, and then the solution was stirred overnight in a nitrogen atmosphere. The precursor was filtered through a 0.45 μm polytetrafluoroethylene (PTFF) filter before use.

2.3. Fabrication of *p-i-n* type perovskite solar cells

ITO glass slides were cleaned by ultrasonification in detergent, water, acetone, ethanol and isopropyl alcohol for 15 min each time. After being dried, the cleaned ITO substrates were treated with ultraviolet ozone for 20 min to make a hydrophilic surface. The ratio of nanocrystals to the PEDOT:PSS (Clevios P VP AI 4083) could be adjusted by the different contents of AuAg ANCs in the solution and the solution were filtrated with a 0.45 μm filter before use. For comparison, a PEDOT:PSS solution without AuAg ANCs was also been prepared. The films were obtained by spin-coating on the ITO substrates at 5000 rpm for 40s and annealing at 150 °C for 15 min in air. Sequentially, the perovskite precursor was coated atop HTL at 3000 rpm for 50 s in glove box. The perovskite film was thermally annealed at 95 °C for 80 min. 15 mg/mL $PC_{61}BM$ in chloroform was spin-coated at 1200 rpm for 60 s atop the perovskite layer. At last, LiF (1 nm) and Al (80 nm) were deposited under vacuum at 1×10^{-6} Torr and a shadow mask was applied to define the active area.

2.4. Characterization

The morphology of AuAg ANCs was obtained by the transmission electron microscopy (TEM, JEOL JEM-2100F, Japan) at an acceleration voltage of 200 kV. Absorption and transmittance spectra were measured on a Cary 5000 instrument (Agilent, USA). The configuration of device was obtained by scanning electron microscopy (SEM, S-4700, Hitachi, Japan). The surface morphologies were recorded by atomic force microscopy (AFM, Bruker USA). The thickness of the PEDOT:PSS layer without and with AuAg ANCs was measured by a spectroscopic ellipsometer (M-2000 V, J.A. Woollam Co., USA). The current density-voltage (*J-V*) curves were recorded on a Keithley 2400 source meter unite under simulated air mass 1.5 global (AM 1.5G) solar irradiation at 100 mW/cm^2 (SAN_EI ELECTRIC, XEC-300M2, Japan). The incident photon-to-current efficiency (IPCE) was collected on a QE-R3011 system (Enli Technology Co., Ltd., China) in air. Both the illumination intensities of the light sources were calibrated by a standard silicon solar cell for reference. The characterizations of the alternating current impedance spectroscopy (ACIS) were acquired by IM6 electrochemical workstation (Zahner Zennium, Germany) with a bias voltage near the respective V_{oc} in the dark condition. The effective area of the cell was 0.1842 cm^2. The impedance spectra parameters were analyzed by Z-view software. The measurements of steady-state photoluminescence (PL) were conducted on FLS980 (Edinburgh Instrument, UK). Time-resolved PL spectra were recorded on LifeSpec (Edinburgh instrument, UK) by exciting with a 477 nm laser (5 MHz).

3. Results and discussion

The AuAg ANCs were synthesized following previously reported method [51] and characterized by TEM and UV–vis spectrum. Fig. 1a shows the TEM image of AuAg ANCs. The size of the AuAg ANCs was 46 nm with deviation of 10.9%, indicating that the ANCs were relatively uniform. The UV–vis absorption spectrum of AuAg ANCs (Fig. 1b) presented an intensive characteristic absorption peak at 428 nm. In this study, the AuAg ANCs were doped into the PEDOT:PSS layer as HTL. As shown in Fig. 1c, the device configuration adopted was ITO/AuAg ANCs@PEDOT:PSS/$MAPbI_{3-x}Cl_x$/$PC_{61}BM$/LiF/Al. Fig. 1d displays the cross-sectional SEM image of the device. Each layer of the device was marked with different colors, and original cross-sectional SEM image was given in Fig. S1.

It was reported that the plasmonic excitation wavelength was closely related to the size of the metal nanocrystals doped into the layer. Additionally, the bigger nanocrystals had a larger scattering cross-section which could reduce absorption loss, but could be detrimental to the charge transport [46]. Therefore, an appropriate size of AuAg ANCs in the PEDOT:PSS layer of pero-SCs was crucial. The size of AuAg ANCs determined by TEM image was ∼46 nm, which was comparable to the thickness of the PEDOT:PSS layer (∼54 nm) and was likely to be beneficial for the scattering effect. Besides, the thickness of the AuAg ANCs@PEDOT:PSS layer was ∼50 nm, which didn't change significantly. Therefore, most of the AuAg ANCs could be possibly imbedded within PEDOT:PSS layer and some AuAg ANCs were exposed on the surface [47]. This assumption was further confirmed by AFM images. Fig. 2a and b shows the surface morphology of the PEDOT:PSS layer without and with AuAg ANCs. The AFM images showed that the root-mean-squared (RMS) roughness of PEDOT:PSS layer was 1.7 nm, while the RMS of AuAg ANCs@PEDOT:PSS layer was 2.5 nm. The RMS difference was very possibly caused by the high frequency fluctuations contributed by the AuAg ANCs exposed on the surface. UV–vis